



## **EXPERIMENTAL STUDY ON ULTIMATE SHEAR STRENGTH OF INTERIOR BEAM-COLUMN JOINTS OF STEEL AND REINFORCED CONCRETE STRUCTURE**

**Atsunori KITANO<sup>1</sup>, Osamu JOH<sup>2</sup> and Yasuaki GOTO<sup>3</sup>**

### **SUMMARY**

Experimental studies were carried out to clarify the stress-transfer mechanism of Steel and Reinforced Concrete (SRC) beam-column joints. Variables of the experiment were the cross-sectional shape of the steel column, concrete strength and eccentricity of the beams for the column. All SRC specimens failed in joint shear. The experimental results showed. 1) Destruction of the eccentric joint differed greatly between the beam eccentricity side and the opposite side. The reduction of shear strength for SRC beam-column joints caused by the eccentricity was smaller than that for RC beam-column joints. 2) Shear strength was also reduced when the transverse beams were eccentrically connected to the column. 3) The effective shear strength of the parallel flanges depended on the reciprocal of the distance from the center of the web to the parallel flanges, when they were located at outside of the RC beam width. 4) The shear resistance shared by the RC joint, and concrete strength were in a linear relation.

### **INTRODUCTION**

Damage to beam-column joints in steel and reinforced concrete (SRC) structures had not been reported before the Hyogo-ken-Nanbu Earthquake of 1995. The authors carried out experimental studies and pointed out that the calculation of the ultimate shear strength of beam-column joints using the Standards for SRC Structures published by the Architectural Institute of Japan (AIJ) [1] did not concur with the experimental values. In addition, the authors showed that the ultimate shear strength of SRC beam-column joints with a steel column cross-section of a cross-H could be estimated from four shear resistance elements: concrete, a joint web plate, parallel flanges in transverse beams and a rectangular frame formed with column and beam flanges. The authors have further proposed a new equation for SRC beam-column joints [2]. However, because of its intricacy, the stress-transfer mechanism of SRC beam-column joints is still not clear. In the present study, experimental studies were carried out to clarify the stress-transfer mechanism of SRC beam-column joints.

---

<sup>1</sup> Instructor, HOKKAIDO University, Sapporo, Japan. Email: kitano@eng.hokudai.ac.jp

<sup>2</sup> Professor, HOKKAIDO University, Sapporo, Japan. Email: joh@eng.hokudai.ac.jp

<sup>3</sup> Associate Professor, HOKKAIDO University, Sapporo, Japan. Email: gottsu@eng.hokudai.ac.jp

## OUTLINE OF THE EXPERIMENT

### TEST SPECIMENS

Nine SRC specimens were used in this study; details are shown in Figure 1 and Table 1. The specimen configuration represented beam and column segments between inflection points in a frame subjected to lateral loading. The contraction scale of the test specimens was about 1/2 of an SRC structure on the assumption of beam-column joints of a middle floor in a multistory multi-span. To make sure that the beam-column joint shear failure occurs prior to any other failure; the joint shear strength was designed smaller than the flexural and shear strengths of the beam and column. Experimental variables were transverse flange thickness, cross H-section of the steel column, concrete strength, column width, column depth and eccentricity of the beams for the column. Specimen SRC-1-W, has been reported previously, and was used as a standard for all specimens. Specimen SRC-1-BW16 had a transverse flange thickness of 16mm. Specimen SRC-7 had no transverse web and flanges, so its steel section of column was an H-section in which web thickness was 12mm. Specimen SRC-8-W had transverse flanges located outside of the SRC beam width. Specimens of the SRC-11-series had a 500mm column depth; and SRC-11-WE had transverse flanges assuming the eccentricity of transverse beams. Specimens of the SRC-12-series had a 500mm column width; and SRC-12-WE had eccentric beams for the column. The SRC-1-WH-series used high strength concrete. The design strength of the concrete was set at  $60\text{N/mm}^2$  (SRC-1-WH8) and  $70\text{N/mm}^2$  (SRC-1-WH9); and set at  $30\text{N/mm}^2$  in the other test specimens. The arrangements of the main column reinforcement bars were 16-D10 for the SRC-11-series and SRC-12-series, and 12-D10 for the other specimens. The arrangements of the beam main reinforcement bars were 8-D19 for the SRC-1-WH9,

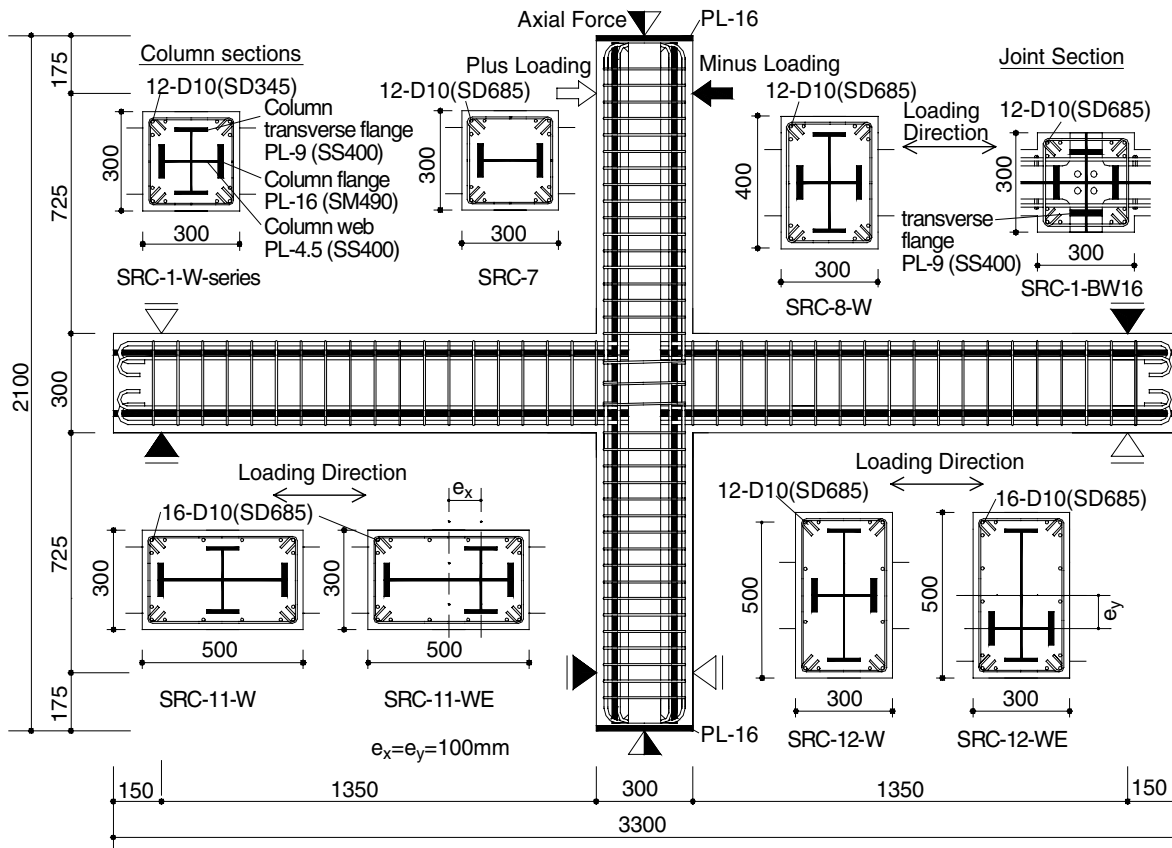


**Figure 1. Outline of the specimens**

8-D13 for the SRC-11-series, and 4-D13 on the first layer and 4-D10 on the second layer for the other specimens. The shear reinforcement of all members used 6 $\phi$ . All specimens also had flanges of 16mm thickness and web of 4.5mm thickness for the columns and beams. The thickness of the transverse flanges of all specimens except for SRC-1-BW16 and SRC-7 were 9mm. Material properties are shown in Table 2-a, 2-b and 2-c.

**Table 1. Outline of the specimen**

specimen	variation	column					beam				joint		
		width( $c_b$ )x depth( $cD$ ) mm	shear reinf. ratio ( $w\rho$ ) %	steel bar	steel		width( $b_b$ )x depth( $bD$ ) mm	shear reinf. ratio ( $w\rho$ ) %	steel bar	steel	shear reinf. ratio ( $w\rho$ ) %	steel	
					L.D.	T.D.						L.D.	T.D.
SRC-1-W*	standard	300x300		B	①	④	200x300	0.37	a	①	0.19	①	④
SRC-1-BW16	transverse flange thickness	300x300	0.37	A	①	①	200x300	0.37	b	①	0.19	①	①
SRC-7	H-section in column steel				②	-						②	-
SRC-1-WH8	high strength concrete	400x300	0.28	A	①	④	200x300	0.37	c	①	0.14	①	④
SRC-8-W	position of t.f.				⑤	⑤						⑤	⑤
SRC-11-W	column depth	300x500	0.37	C	③	④	200x300	0.37	b	①	0.19	③	④
SRC-11-WE	eccentricity of t.f.	500x300	0.22		①	⑥						200x300	0.37
SRC-12-W	column width			300x300	0.37	A	④	④	200x300	0.37	d		
SRC-12-WE	eccentricity of loading beam	300x300	0.37				A	④				④	200x300
SRC-1-WH9	high strength concrete			300x300	0.37	A		④	④	200x300	0.37	d	

NOTE: \* : The specimen of previous report, L.D. : Loading Direction, T.D. : Transverse Direction, t.f. : transverse flange

shape of steel H-section	column steel bar	beam steel bar
① : BH-200x100x4.5x16	A : 12-D10(SD685)	a : 4-D13(SD1000equ.) .4-D10(SD800equ.)
② : BH-200x100x12x16	B : 12-D10(SD685)	b : 4-D13(SD685) .4-D10(SD685)
③ : BH-400x100x4.5x16	C : 16-D10(SD685)	c : 8-D13(SD1000equ.)
④ : BH-200x100x4.5x9		d : 8-D19(SD785)
⑤ : BH-300x100x4.5x9		equ. : equivalent
⑥ : BH-400x100x4.5x9		

**Table 2-a. Mechanical properties of steel bar**

specimen	steel	yield stress $\sigma_y$ (N/mm <sup>2</sup> )	yield strain $\epsilon_y$ ( $\mu$ )	Young's modulus $E$ (kN/mm <sup>2</sup> )
SRC-1-BW16	D13(SD685)	729	4050	180
SRC-7	D10(SD685)	720	4600	158
SRC-8-W	6 $\phi$ (SR345eq.)	415	2130	195
SRC-1-WH8				
SRC-11-W	D19(SD700)	807	4420	183
SRC-11-WE	D13(SD1000eq.)	967	5050	191
SRC-12-W	D13(SD685)	729	3780	193
SRC-12-WE	D10(SD685)	707	3870	183
SRC-1-WH9				
SRC-1-WH9	6 $\phi$ (SR345eq.)	378	2170	175

**Table 2-b. Mechanical properties of steel plate**

specimen	steel plate	yield stress $\sigma_y$ (N/mm <sup>2</sup> )	yield strain $\epsilon_y$ ( $\mu$ )	Young's modulus $E$ (kN/mm <sup>2</sup> )
SRC-1-BW16	PL-16	361	1890	192
SRC-7	PL-12	320	1600	200
SRC-8-W	PL-9	290	1550	188
SRC-1-WH8	PL-4.5	310	1630	190
SRC-11-series	PL-16	381	2050	186
SRC-12-series	PL-9	305	1590	193
SRC-1-WH9	PL-4.5	301	1480	205

eq. : equivalent reinf. : reinforcement

**Table 2-c. Mechanical properties of concrete**

specimen	compressive stress $\sigma_B$ (N/mm <sup>2</sup> )	tensile stress $\sigma_t$ (N/mm <sup>2</sup> )	compressive strain $\epsilon_{max}$ ( $\mu$ )	Young's modulus $E_{1/3}$ (kN/mm <sup>2</sup> )	Young's modulus $E_{2/3}$ (kN/mm <sup>2</sup> )
SRC-1-W	34.4	2.98	3050	23.7	20.1
SRC-1-BW16	30.6	1.84	2830	23.5	19.6
SRC-7	36.2	2.60	3070	24.3	20.7
SRC-1-WH8	62.5	3.79	2390	32.0	29.8
SRC-8-W	38.7	2.80	2540	27.0	23.8
SRC-11-W	37.5	2.24	2360	29.0	26.3
SRC-11-WE	36.7	3.06	2830	25.8	22.2
SRC-12-W	43.3	3.14	2760	28.0	24.4
SRC-12-WE	42.8	3.40	2880	27.6	24.0
SRC-1-WH9	72.2	4.01	2690	32.1	30.9

**LOADING AND INSTRUMENTATION**

Loading arrangement is schematically shown in Figure 2. The incremental forced displacement was given to the specimen at the top of the column cyclically during the application of column axial stress of  $\sigma_B/6$ . The loading was controlled at the load of the column until the third cycle, and thereafter it was controlled in the displacement of the column. The value of the peak in the third cycle was set at 80% of the calculated value of ultimate shear strength of the beam-column joint, and the values of the peak until the third cycle were each increased by a 1/3 of the peak value at the third cycle. The value of the peak of the fourth cycle, which was equalized with the displacement of the column of the peak in third cycle, was set at a standard displacement  $\delta$ . The cycles thereafter carried out cyclically loading by displacement control so that the peak displacement could become n (n=2,3,4,6,8) times  $\delta$ . During the tests, the forces, displacements and reinforcement strains were measured.

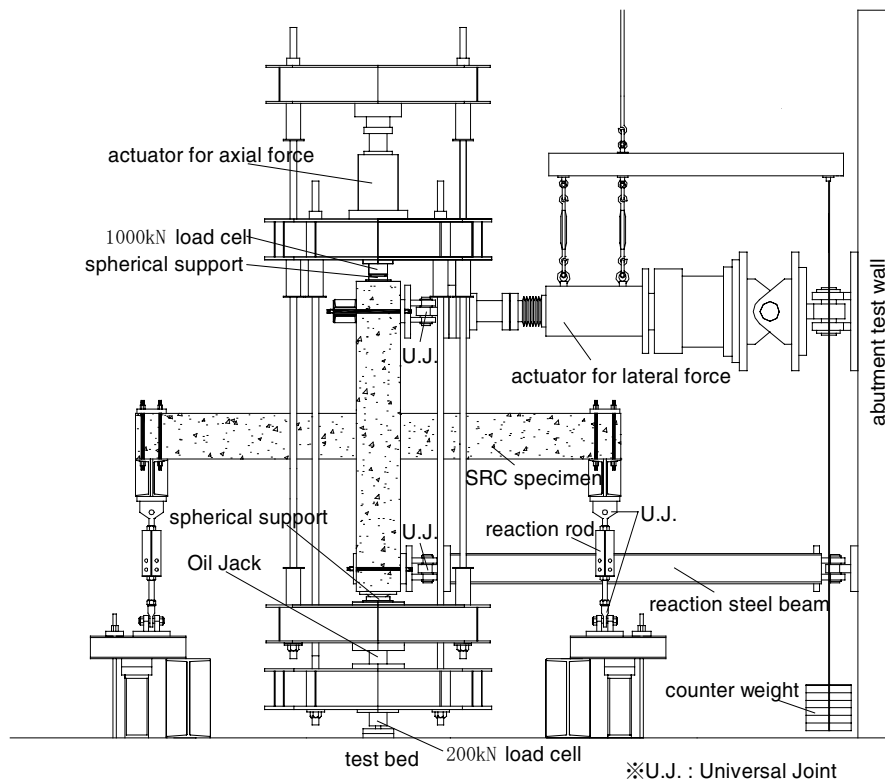


**Figure 2. Outline of the loading equipment**

## TEST RESULTS AND DISCUSSION

### CIRCUMSTANCES OF FAILURE

The circumstances of the failures for some specimens after testing are shown in Figure 3. The general process of cracking was as follows. An initial flexural crack appeared in the beam end during the first cycle loading, and initial joint shear cracks appeared up to about the third cycle loading. After that, shear cracks markedly appeared in most parts in the joint by the fifth cycle. The widening of the shear crack of the joint was intensified after the seventh cycle, and the concrete cover came off in places. Most joint shear cracks were extended to the column with the increase in the displacement. All specimens except SRC-11-W failed in joint shear. For SRC-11-W (column depth of 500mm), the concrete at the end of the beam failed in flexural crushing before the shear crack of the joint markedly appeared, so the fracture mode of this specimen was joint shear failure after flexural crushing failure at the end of the beam. For SRC-1-BW16 (transverse flange thickness of 16mm), most shear cracks appeared at an angle of about 60-degrees, and the delaminating of the concrete around the steel transverse beam was remarkable. For SRC-7 (H shape column steel section), the shear crack appeared concentrated in the central part of the joint, essentially without appearing in the column, and the delaminating of the concrete was less than other specimens. The shear crack appeared at 45-degrees on the diagonal line of the joint. For SRC-1-WH8 (concrete strength of  $64\text{N/mm}^2$ ), the shear crack characteristically appeared in the joint extended for the column, and the crack extended vertically in the column; the flexural crack of the joint was greater than in other specimens. For SRC-11-WE (eccentric transverse flange in the loading direction), a shear crack of a different angle that took the transverse web as its boundary appeared. From this, it was guessed that the

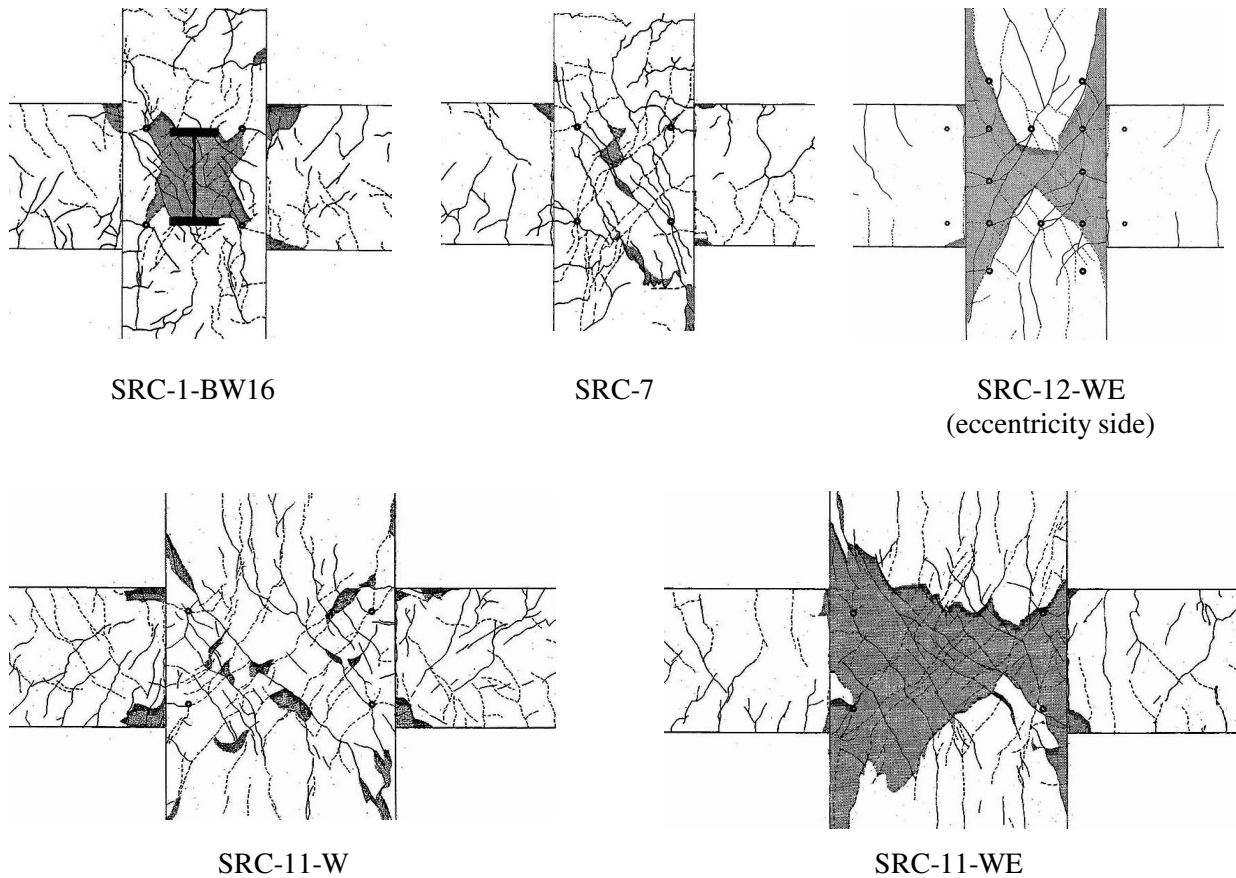


Figure 3. Circumstances of failure

internal stress transfer mechanisms of the concrete right and left of the transverse web respectively differed. For SRC-12-WE (column with an eccentric beam), damage to the concrete was slight, when the plane on the opposite side was compared with the eccentricity side, while the damage to the concrete was more remarkable, as the transverse flange was exposed in the center in the eccentricity side.

### LOAD VS. DISPLACEMENT RELATIONSHIP

Skelton curves of all specimens, which were obtained from the interaction curves of the column shear force ' $cQ$ ' and story deformation angle ' $cR$ ', are shown for comparison in Figures 4 to 6.

#### *Effect of the shape of the transverse flange (Figure 4)*

The effect of the thickness of the transverse flange can be observed by comparing SRC-1-BW16 with the standard specimen SRC-1-W. It has been proven that the maximum strength in SRC-1-BW16 rises greatly, in comparison with the standard specimen, and that the transverse flange bears the shear force. The effect of the position of the transverse flange can be observed by comparing SRC-7 and SRC-8-W, and the standard specimen SRC-1-W. In a comparison between Specimen SRC-7, which had no transverse flanges and web, and the standard specimen SRC-1-W; though the frame stiffness was higher by the fifth cycle in which the appearance of the shear crack became remarkable in the joint, the stiffness reduction rapidly occurred afterwards, and the maximum strength appeared in a story deformation angle that was smaller than the standard specimen. From this fact, it was considered that rapid stiffness reduction could be prevented, even if the RC division was fractured, since the area of the RC division restricted by the presence of the transverse H-section increased. For SRC-8-W (transverse flanges located outside the SRC beam width), though the maximum strength seemed to rise, since the area of the RC division, which surrounded in the steel flanges of the column, increases, the strength reduction was rapid after the maximum strength was reached.

#### *Effect of column width, column depth and the eccentricity of the beam (Figure 5)*

In respect to the effect of column depth; though initial stiffness of the frames were high, when SRC-11-W and SRC-11-WE, which had a column depth of 500mm, were compared with the standard specimen SRC-1-W, the maximum strengths appeared at a small story deformation angle, and strength reductions were rapid after the maximum strength was reached. Though the frame strength for shear fracture leveled off after a beam flexural crushing failure for SRC-11-W, frame strength was rapidly reduced after the RC

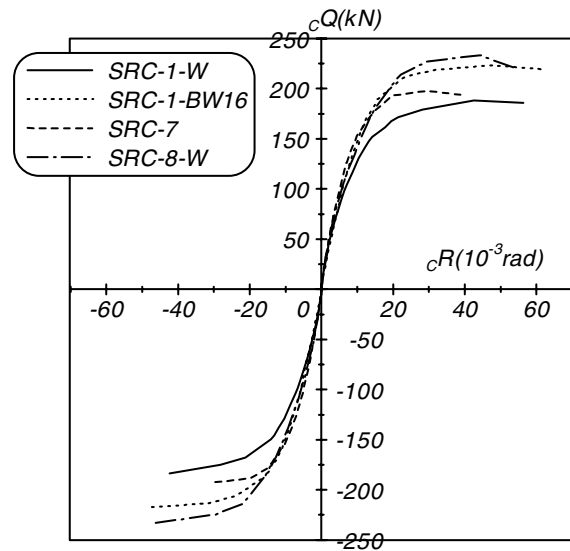


**Figure 4. Skelton curves  
(Effect of the shape of the transverse flange)**

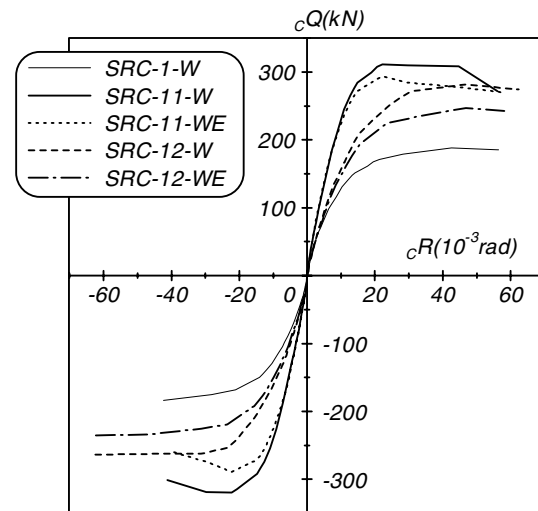


**Figure 5. Skelton curves  
(Effect of column width, column depth  
and the eccentricity of the beam)**

division in the joint was fractured by the shearing stress. In comparisons between the SRC-12-series (column width of 500mm) and the standard specimen SRC-1-W, the maximum strength of the SRC-12-series was raised more than the standard specimen, since the column width was wide; however, frame stiffnesses were almost the same, and strength reduction after the maximum strength was reached was also small. In respect to the effect of the eccentricity, for SRC-11-WE, in which the transverse beam was eccentric in the loading direction, the stiffness reduction was larger than SRC-11-W as non-eccentricity and maximum strength also decreased; and the strength reduction after the maximum strength was reached was also large. For SRC-12-WE, in which the beam in the loading direction was eccentric, though the initial stiffness was the same as SRC-12-W, non-eccentric, the strength increase after the stiffness reduction was small, and the maximum strength also decreased. However, the transition of the load and deformation relationship after the maximum strength was reached was similar regardless of being eccentric or non-eccentric.

#### Effect of concrete strength (Figure 6)

In comparisons between the specimens (SRC-1-WH-series) using high strength concrete and the standard specimen (SRC-1-W) using usual strength concrete; though the stiffness of the frame was higher, as the concrete strength was higher, the story deformation angle at the maximum strength was smaller, and the strength reduction after the maximum strength was reached was larger.

### SHEAR STRENGTH

#### Shear strength in the initial shear crack of the joint

The calculated values of the strengths at the initial shear crack of the joint for all specimens were calculated from the AIJ-SRC Standard equation; the experimental values are shown in Table 3. The experimental and calculated values were compared for the joint shear force ( ${}_jQ$ ). At the AIJ- SRC Standard, the design aim, in the sustained loading of a beam-column joint, is that an oblique crack does not appear at the beam-column joint; and the calculation formula of the strength of a joint shear initial crack is given in the equation as follows.

$${}_jQ_{cr} = {}_c\tau_{cr} \cdot {}_cb \cdot {}_{mC}d \cdot (1 + \beta) \quad (1)$$

Where,

$${}_c\tau_{cr} = 0.1\sigma_B$$

$$\beta = \frac{15 {}_jt_w \cdot {}_sCd}{{}_cb \cdot {}_{mC}d}$$

- Symbols:  ${}_jQ_{cr}$  : shear strength in the initial shear crack of joint (kN)  
 ${}_c\tau_{cr}$  : Shear stress as the crack appears in the concrete (N/mm<sup>2</sup>)  
 ${}_cb$  : Column width (mm)  
 ${}_{mC}d$  : Distance between columns main reinforcement (mm)  
 $\beta$  : Coefficient by shape and dimension of the steel web member  
 $\sigma_B$  : Concrete strength (N/mm<sup>2</sup>)  
 ${}_jt_w$  : Web thickness of the joint (mm)  
 ${}_sCd$  : Distance between centers of gravity of the column steel flange (mm)

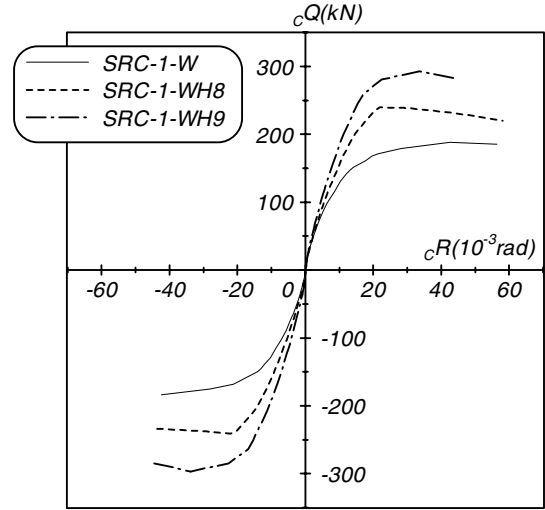


Figure 6. Skelton curves  
(Effect of concrete strength)

**Table 3. Shear strengths in initial shear crack of beam-column joints**

specimen	shear strength in initial shear crack of joint ${}_J Q_{cr}$							
	exp(kN)		cal1	cal2	exp/cal1		exp/cal2	
	+	-	(kN)	(kN)	+	-	+	-
SRC-1-W	371	236	263	356	1.41	0.90	1.04	0.66
SRC-1-BW16	481	568	234	381	2.06	2.43	1.26	1.49
SRC-7	535	127	351	351	1.52	0.36	1.52	0.36
SRC-1-WH8	134	468	477	646	0.28	0.98	0.21	0.72
SRC-8-W	468	515	378	483	1.24	1.36	0.97	1.07
SRC-11-W	906	952	562	663	1.61	1.69	1.37	1.43
SRC-11-WE	661	595	550	649	1.20	1.08	1.02	0.92
SRC-12-W	608	608	515	632	1.18	1.18	0.96	0.96
SRC-12-WE	608	435	509	625	1.19	0.85	0.97	0.70
SRC-1-WH9	538	461	551	746	0.98	0.84	0.72	0.62
average					1.27	1.17	1.00	0.89

In the above equation, when the coefficient  $\beta$  from the shape and dimension of the steel web member is calculated, only sectional-area of the steel web is considered, even if there are the transverse flanges and so on. However, because cruciform steel from which the H-section steel was orthogonally combined was used for the column steel in all specimens except SRC-7, the calculated values (cal2) including the sectional-area of the transverse flanges are also shown in Table 3. Further, cal1 in the table is a value calculated considering only the joint steel web. The mean value of the ratio of the calculated and experimental values was 1.30 in the positive pressurization, when the transverse flange was not considered, and it was 1.03 on positive pressurization, when the transverse flange was considered so it comparatively well corresponded to the case when the transverse flange was considered. However, the calculated values in specimens using high strength concrete had a tendency of overestimating the experimental values, which seemed to decrease further than the calculated ones, because the concrete tensile strength in the specimen using high strength concrete was overestimated.

#### *Ultimate Shear strength of the joint*

Table 4 shows a comparison of the experimental and calculated values using the AIJ-SRC standard equation [1], and that using the proposed equation of authors [2]. The AIJ-SRC standard and proposed equations are shown following. Though the AIJ-SRC standard is not an equation that considers the transverse flange; in this study, the calculated values were obtained by the inclusion of the transverse flange section product in the steel web sectional-area.

AIJ-SRC Standard:

$$\begin{aligned}
 {}_J Q_U &= {}_J M_U / {}_{mb} d \\
 {}_J M_U &= {}_c V_e ({}_J F'_s \cdot {}_J \delta + {}_w p \cdot {}_w \sigma_Y) + \frac{1.2 {}_s V \cdot {}_s \sigma_Y}{\sqrt{3}} \quad (2)
 \end{aligned}$$

Where,

$$\begin{aligned}
 {}_c V_e &= \frac{{}_c b + {}_B b}{2} {}_{mB} d \cdot {}_{mC} d, \quad {}_s V = {}_J t_w \cdot {}_s B d \cdot {}_s C d \\
 {}_J F'_s &= \min \left( 0.12 F_c, 1.8 + \frac{3.6 F_c}{100} \right), \quad {}_J \delta = 3(\text{cross-shaped}), 2(\text{T-shaped}), 1(\text{L-shaped})
 \end{aligned}$$

Proposed equation by authors:

$${}_J Q_U = {}_C A \times 0.39 \sigma_B + {}_w Q_J + 0.9 {}_f Q_J + 0.5 {}_{fr} Q_J \quad (3)$$

Where,

$${}_w Q_J = \frac{s_w \sigma_y}{\sqrt{3}} \cdot A_w, \quad {}_f Q_J = \frac{f \sigma_y}{\sqrt{3}} \cdot A_f$$

$${}_{fr} Q_J = \left( \alpha \cdot b_{fr} \cdot t_{fr}^2 \cdot {}_{fr} \sigma_y / 4 \right) / {}_{mB} d$$

Symbols:

- ${}_J M_U$ : ultimate shear strength of beam-column joint converted into the moment
- ${}_c V_e$ : effective volume of the concrete part of beam-column joint
- ${}_s V$ : volume of the steel web of beam-column joint
- ${}_J F_s$ : shear strength of the concrete of beam-column joint.
- ${}_J \delta$ : shape factor of beam-column joint
- ${}_C b$ : column width,  ${}_B b$ : beam width
- ${}_{mB} d$ ,  ${}_{mC} d$ : distance between main reinforcement of top and bottom of beam or column
- ${}_{sB} d$ ,  ${}_{sC} d$ : distance between centers of gravity of the steel flange of beam or column
- ${}_J t_w$ : thickness of steel web plate of beam-column joint
- ${}_w p$ : shear reinforcement ratio
- ${}_w \sigma_Y$ : yield stress of shear reinforcement
- ${}_s \sigma_Y$ : yield stress of steel plate
- $F_c$ ,  $\sigma_B$ : compressive stress of the concrete
- ${}_C A$ ,  $A_w$ ,  $A_f$ : sectional-area of concrete, web plate, flange plate
- $b_{fr}$ ,  $t_{fr}$ : width or thickness of flange plate of column and beam

The mean value of the ratio of the value calculated by the AIJ-SRC standard equation and the experimental value was 1.31; therefore, it seemed that the values calculated by the AIJ-SRC standard equation overestimated the experimental values. Whereas it was 0.99 using the proposed equation; consequently, it was clear that the values calculated by the proposed equation agreed reasonably well with the experimental ones.

It was shown that the proposed equation's calculated values agreed with the experimental ones, when the

**Table 4 : The comparison of calculated value and experimental value**

specimen	Ultimate shear strength of beam-column joints ${}_J Q_U$								
	$\sigma_B$ (N/mm <sup>2</sup> )	exp(kN)		cal1 (kN)	exp/cal1		cal2 (kN)	exp/cal2	
		plus	minus		plus	minus		plus	minus
SRC-1-W	34.4	1280	1250	1030	1.24	1.21	1210	1.06	1.03
SRC-1-BW16	30.6	1520	1480	1300	1.17	1.14	1380	1.10	1.07
SRC-7	36.2	1350	1310	965	1.40	1.36	1200	1.13	1.09
SRC-1-WH8	62.5	1630	1640	1160	1.41	1.41	1760	0.93	0.93
SRC-8-W	38.7	1590	1590	1120	1.42	1.42	1430	1.11	1.11
SRC-11-W	37.5	1400	1280	968	1.45	1.32	2150	0.65	0.60
SRC-11-WE	36.7	1210	1200	1050	1.15	1.14	2110	0.57	0.57
SRC-12-W	43.3	2100	2150	1740	1.21	1.24	1740	1.21	1.24
SRC-12-WE	42.8	1980	1950	1730	1.14	1.13	1720	1.15	1.13
SRC-1-WH9	72.2	1920	1800	1260	1.52	1.43	1980	0.97	0.91
				average	1.31	1.28	average	0.99	0.97

NOTE: cal1=AIJ-SRC standard, cal2=proposed by authors

inside steel was changed even to H-section steel of cruciform section steel, because the correspondence of the experimental and calculated values using the proposed equation was good for SRC-7 that had H-section inside steel. For SRC-12-W and SRC-8-W, since the transverse flanges existed outside the SRC beam width, it was anticipated that the shear force of the transverse flanges decreased further than in the case where they were in the beam width. However, it was found that the transverse flange, even if it exists outside of the SRC beam width, bore a shear force equivalent to the case in which it is in the beam width; because the correspondence of the ratio of the calculated values by the proposed equation and experimental value was also good for both specimens. For SRC-12-W and SRC-11-W, it was confirmed that the proposed equation appropriately evaluated the experimental value even in the case of a flat section column in which the column depth or column width extended; because the good correspondence of the experimental value and the calculated value of the proposed equation. As for SRC-12-WE, in which the beam was eccentric for the column, the experimental value decreased further, by about 14%, than in SRC-12-W in which the beam was not eccentric, and the maximum strength was lowered by the eccentricity. Calculated values where the beam is eccentric for the column, and where the beam is not eccentric, were the same for both the AIJ-SRC standard and the proposed equations, since the effective width is also given in the average of the column and beam widths. The effective width should be considered in an SRC structure, as well as the RC and NZ standards, for which eccentricity is considered in order to reduce seismic damage on the eccentric side; this because, when beams were eccentric to the column, there was much damage to joints in Hyogo-ken Nanbu Earthquake 1995. The experimental value decreased a little more in SRC-11-WE, in which the orthogonal beam was eccentric, than for SRC-11-W in which the transverse beam was not eccentric. Since SRC-11-W had joint shear failure after the flexural collapse at the end of beam, it is considered that the maximum strength was smaller than when the joint was fractured purely by shearing stress. Therefore, the difference in the shear strength of both joints seems to extend more, and the ultimate shear strength of the joints seems to be lower, when the orthogonal beam is eccentric. Since consideration of eccentricity by the effective width is not possible, as in the case in which the loading beam is eccentric, it is necessary to consider the lowering of the ultimate strength by the eccentricity of the transverse beam, such as by a strength calculation equation multiplying the reduction coefficient of the eccentricity proportion. For SRC-1-WH8 and SRC-1-WH9, using high-strength concrete, it was clarified that the shear strength in the concrete division calculated by the AIJ-SRC standard equation had overestimated the experimental values; whereas the calculated values using the proposed equation had well evaluated the experimental ones.

The relationship between concrete strength ( $\sigma_B$ ) and shear stress of an RC division ( ${}_{rc}Q$ ), which deduced the experimental value of a steel specimen from the value of the ultimate strength of an SRC specimen, is shown in Figure 7. In all specimens, the experimental values of the shear strength exceeded the ones calculated by the AIJ-SRC standard equation; and especially, the difference of the calculated and experimental values increased in specimens using high strength concrete. However, the proposed equation, which had linearly evaluated shear strength and concrete strength, agreed reasonably well with the experimental values. From this fact, it was clarified that there was a linear relation in the shear strength shared by the RC, and the concrete strength, if the concrete strength is within about 70N/mm<sup>2</sup>.

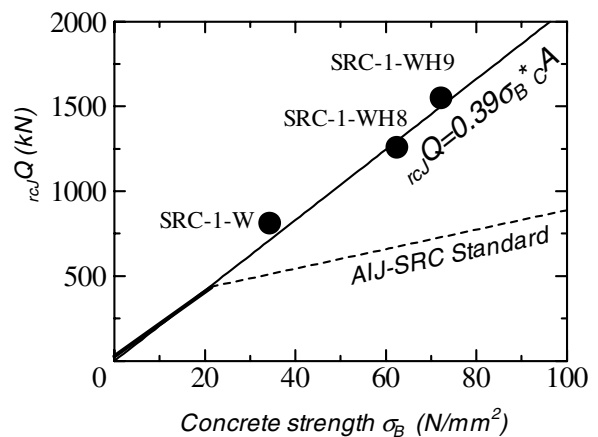


Figure 7. Relationship between  $\sigma_B$  and  ${}_{rc}Q$

The relationship between the experimental values and those calculated by the AIJ-SRC standard equation, and those by the proposed equation, including specimens examined in other research institutes are shown in Figure 8, and statistical data are shown in Table 5. Since the mean value of the ratio of the experimental value and those calculated by the AIJ-SRC standard equation was 1.28; the AIJ-SRC standard equation had overestimated the ultimate strength of the beam-column joints. However, the mean value of the ratio of the values calculated by the proposed equation, which evaluated concrete, web, transverse flange and frame effects as shear resistance elements, and the experimental values, approximated 1.00, and the dispersion was also improved. Thus, the validity of the proposed

**Table 5. The statical data of the ratio of the calculated and the experimental values**

	AIJ-SRC	Proposed
number of specimens	28	28
average	1.28	1.02
standard deviation	0.20	0.12
coefficient of variation	0.16	0.12

equation was confirmed.

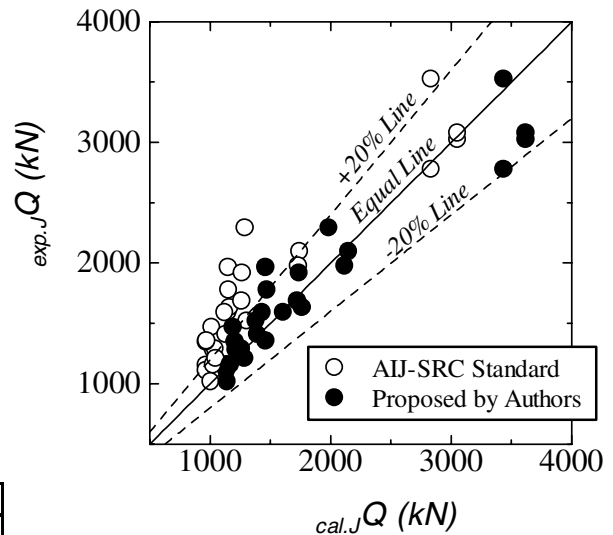


**Figure 8. Relationship between the calculated and the experimental values**

## CONCLUSIONS

The following observations were obtained from the lateral load reversal tests performed on beam-column joint specimens of SRC structures.

- 1) The destruction of the eccentric joint differed greatly between a beam's eccentricity side and its opposite side. The reduction of shear strength for SRC beam-column joints caused by the eccentricity was smaller than that for RC beam-column joints.
- 2) Shear strength was also reduced when the transverse beams were eccentrically connected to the column.
- 3) The effective shear strength of the parallel flanges depended on the reciprocal of the distance from the center of the web to the parallel flanges, when they were located from outside of the RC beam width.
- 4) The shear resistances shared by the RC joint and concrete strength were in a linear relation.

## REFERENCES

1. Architectural Institute of Japan, "Standard for Structural Calculation of Steel Reinforced Concrete Structures", 2001 (in Japanese)
2. A.Kitano, O.Joh and Y.Goto, "Investigation on Stress-Transfer Mechanism of SRC Interior Beam-Column Joints", 12<sup>th</sup> World Conference on Earthquake Engineering, Auckland, 2000, Paper ID:1835